

1 **Central carbon metabolism is an intrinsic factor for optimal replication of a norovirus**

2 Karla D. Passalacqua<sup>a</sup>, Jia Lu<sup>b</sup>, Ian Goodfellow<sup>b</sup>, Abimbola O. Kolawole<sup>a</sup>, Jacob R. Arche<sup>a</sup>,

3 Robert J. Maddox<sup>a</sup>, Mary X.D. O’Riordan<sup>a</sup>, Christiane E. Wobus<sup>a#</sup>

4

5 <sup>a</sup>Department of Microbiology and Immunology, University of Michigan, Ann Arbor, Michigan,

6 USA

7 <sup>b</sup>Division of Virology, Department of Pathology, University of Cambridge, Cambridge, UK.

8

9 Running head: Macrophage metabolic response to murine norovirus

10

11 #Address correspondence to Christiane E. Wobus, [cwobus@umich.edu](mailto:cwobus@umich.edu)

12

13 Abstract word count: 227

14 Manuscript word count: 4830

15

16

17 **ABSTRACT**

18 The metabolic pathways of central carbon metabolism, glycolysis and oxidative phosphorylation  
19 (OXPHOS), are important host factors that determine the outcome of viral infections and can  
20 therefore be manipulated by some viruses to favor infection. However, mechanisms of metabolic  
21 modulation and their effects on viral replication vary widely. Herein, we present the first  
22 metabolomics profile of norovirus-infected cells, which revealed increases in glycolysis,  
23 OXPHOS, and the pentose phosphate pathway (PPP) during murine norovirus infection.  
24 Inhibiting glycolysis with 2-deoxyglucose (2DG) in transformed and primary macrophages  
25 revealed that host cell metabolism is an important factor for optimal murine norovirus (MNV)  
26 infection. 2DG affected an early stage in the viral life cycle after viral uptake and capsid  
27 uncoating, leading to decreased levels of viral protein translation and viral RNA replication. The  
28 requirement of central carbon metabolism was specific for MNV (but not astrovirus) infection,  
29 independent of the Type I interferon antiviral response, and unlikely to be due to a lack of host  
30 cell nucleotide synthesis. MNV infection increased activation of the protein kinase Akt, but not  
31 AMPK, two master regulators of cellular metabolism, suggesting Akt signaling may play a role  
32 in upregulating central carbon metabolism during norovirus infection. In conclusion, our findings  
33 suggest that the metabolic state of target cells is an intrinsic host factor that determines the extent  
34 of norovirus replication and implicates metabolism as a virulence determinant. They further  
35 implicate cellular metabolism as a novel therapeutic target for norovirus infections and  
36 improvements of current human norovirus culture systems.

37

38 **IMPORTANCE**

39 Viruses depend on the host cells they infect to provide the machinery and substrates for  
40 replication. Host cells are highly dynamic systems that can alter their intracellular environment  
41 and metabolic behavior, which may be helpful or inhibitory for an infecting virus. In this study,  
42 we show that macrophages, a target cell of murine norovirus (MNV), increase central carbon  
43 metabolism upon viral infection, which is important for early steps in MNV infection. Human  
44 noroviruses (hNoV) are a major cause of gastroenteritis globally, causing enormous morbidity  
45 and economic burden. Currently, no effective antivirals or vaccines exist for hNoV, mainly due  
46 to the lack of high efficiency *in vitro* culture models for their study. Thus, insights gained from  
47 the MNV model may reveal aspects of host cell metabolism that can be targeted for improving  
48 hNoV cell culture systems and for developing effective antiviral therapies.

49

50 **Key words.** *Caliciviridae*, norovirus, metabolism, glycolysis, oxidative phosphorylation,  
51 pentose phosphate pathway

52

53

54

55

## 56 INTRODUCTION

57 Viruses are obligate intracellular parasites. Thus, their biology is entirely dependent on  
58 the physiology of the host cells they infect. One increasingly appreciated aspect of virus-host  
59 interaction is cellular metabolism (1-4). Historically, cellular metabolism has been considered  
60 mainly in terms of its role in cellular energy homeostasis. However, metabolism and metabolic  
61 “cross talk” are increasingly being appreciated as crucial aspects in a range of cellular processes  
62 such as proliferation and cell death (5), the activation and functioning of the immune system (6,  
63 7), autophagy (8, 9) and in the establishment of infectious disease (10). Indeed, a wide range of  
64 pathogens including parasites (11), bacteria (12-14) and viruses (3) have been shown to affect  
65 and to be affected by their hosts’ metabolic activity. Of note, the controlled modulation of  
66 metabolism in immune cells has been shown to be a key feature in adaptive and innate immune  
67 responses (6, 14-16), and these findings have given rise to an entire field referred to as  
68 “immunometabolism” (17-20). For example, macrophages adapt to a variety of metabolic  
69 profiles depending upon the specific signals they sense (21, 22). Specifically sensing through  
70 different Toll-Like Receptors (TLR) in myeloid cells can initiate any combination of up- and/or  
71 down-regulation of glycolysis and OXPHOS (23). Thus, metabolic processes are a vital feature  
72 of the immune system for effectively combating viral infections, or an Achille’s heel of the host  
73 cell that can be manipulated by invading pathogens for their own advantage.

74 Eukaryotic cellular metabolism encompasses a wide range of catabolic and anabolic  
75 processes, and various aspects of host metabolism have been linked to viral infections. In  
76 particular, the major pathways of central carbon metabolism, glycolysis and oxidative  
77 phosphorylation (OXPHOS), have been investigated for their role in viral infection. For  
78 example, Kaposi’s sarcoma herpesvirus (KSHV) suppresses aerobic glycolysis and OXPHOS to

79 foster cellular, and thus viral, survival (24). In contrast, an array of diverse viruses such as herpes  
80 simplex virus 1, HIV-1, rubella virus, white-spot syndrome virus, dengue virus, rhinovirus,  
81 hepatitis C virus, influenza virus, and adenovirus (25-33) have been shown to initiate a host cell  
82 response characterized by an increase in glycolysis, resulting in a more hospitable intracellular  
83 environment for viral replication. However, the specific ways in which viral infections initiate  
84 metabolic responses, and how these responses affect viral infection, vary substantially.  
85 Disentangling the unique metabolic responses of host cells upon viral infection, especially in  
86 regard to glycolysis and OXPHOS, may help in the development of broadly acting antiviral  
87 therapies.

88 Human noroviruses (hNoV) are non-enveloped, positive-sense, single-stranded RNA  
89 viruses of the *Caliciviridae* family that cause the majority of acute non-bacterial gastroenteritis  
90 globally (34-37). In addition to the public health burden, the economic burden of hNoV  
91 infections is enormous, with global costs estimated at \$60 billion (US\$) annually (35, 36).  
92 Currently, there are no licensed vaccines or antivirals that are effective against hNoV infections.  
93 Although advances have been made in developing *in vitro* model systems for studying hNoV  
94 (38-42), the field still lacks a highly efficient, easy-to-use cell culture model. Therefore, murine  
95 norovirus (MNV) remains a powerful tool for investigating general norovirus biology (43-45).  
96 The goal in the current study was to identify aspects of host cell metabolism that are important  
97 for modulating MNV replication. Such findings may enable the development of more efficient  
98 hNoV culture systems and/or antiviral therapies and vaccines for hNoV in the future (46).

99 With these goals in mind, we performed the first metabolomic analysis of norovirus  
100 infection. Our analysis demonstrated that MNV infection of macrophages causes changes in the  
101 host cell metabolic profile characterized by an increase in central carbon metabolism. Inhibition

102 of glycolysis with 2-deoxyglucose (2DG) severely attenuated MNV, but not human astrovirus  
103 VA1, infection *in vitro*. Inhibition occurred at the level of replication, as we observed a lag in the  
104 appearance of viral proteins in infected cells with a concomitant lag in viral genome replication,  
105 but no effect on viral uptake or uncoating. Inhibition of MNV infection by 2DG was not rescued  
106 by addition of nucleotides and was independent of Type I interferon responses. Investigations of  
107 the two master regulators of cellular metabolism, Akt and AMPK, revealed that MNV infection  
108 caused an increase in Akt activation, while inhibition of Akt signaling reduced both cellular  
109 glycolysis and MNV infection. Overall, our findings identify central carbon metabolism as an  
110 intrinsic host factor important for optimal MNV infection of macrophages. Since noroviruses  
111 have a tropism for immune cells (47) and specific immune cell subsets are characterized by  
112 different metabolic profiles (48, 49), these findings may have implications for viral pathogenesis  
113 and the development of improved hNoV culture systems.

114

115 **RESULTS**

116 *Targeted metabolomics survey identifies multiple metabolites that increase during MNV-1*  
117 *infection in RAW 264.7 cells.*

118       Viral infections can cause changes in host cell metabolism that are important for viral  
119 replication (1, 3). In our efforts to identify host cell factors that are important for successful  
120 norovirus (NoV) infection, we hypothesized that infection of macrophages with murine  
121 norovirus (MNV) causes changes in central carbon metabolism of host cells that are beneficial or  
122 required for optimal viral infection. MNV-1 (CW3 isolate) is an acute strain of murine norovirus  
123 that has a natural tropism for macrophages *in vivo* and is particularly efficient at infecting  
124 transformed murine macrophages RAW 264.7 (RAW) (44). Thus, we performed a targeted  
125 metabolomics profiling of MNV-infected RAW cells to identify changes in the amount of host  
126 cell metabolites from glycolysis, the tricarboxylic acid cycle (TCA) and others.

127       A targeted mass spec analysis of metabolites isolated from MNV-1 infected RAW cells  
128 (MOI=5) after eight hours of infection (approximately one replication cycle) revealed multiple  
129 metabolites that were significantly increased in infected cells compared to mock cells, or  
130 unchanged, but no metabolites that were significantly decreased during infection (**Fig. 1**)  
131 (**Supplemental Tables 1 and 2**). In particular, an increase in select metabolites from glycolysis  
132 (fructose-bisphosphate, 2- and 3-phosphoglycerate, dihydroxyacetone-phosphate), the pentose  
133 phosphate pathway (PPP) (6-phosphogluconate) and the TCA cycle (citrate/isocitrate, malate)  
134 suggest that both energy generating pathways of glycolysis and oxidative phosphorylation are  
135 increased during MNV infection (**Fig. 1A**). Notably, overall levels of ATP were higher in  
136 infected cells compared to mock (**Fig. 1A**), indicating an overall increase in RAW cell  
137 metabolism as a result of viral infection. The detection of a significant increase in metabolites in

138 cell culture is particularly noteworthy, since MNV-infected cultures represent a heterogeneous  
139 population of infected and uninfected cells, since not all cells get infected by MNV even when  
140 experiments are done with a high MOI (50).

141 Another group of metabolites that increased in RAW cells during MNV infection include  
142 inosine-monophosphate (IMP), hypoxanthine and xanthine (**Fig. 1B**). These metabolites are part  
143 of a pathway involved in adenosine catabolism that can result in the production of uric acid, a  
144 potent immune signal (16), and potentially reactive oxygen intermediates, which can have  
145 signaling and antimicrobial activity. Upregulation of enzymatic activity in this pathway and an  
146 increase in the resulting metabolites has been observed in the liver of mice infected with several  
147 RNA and DNA viruses (51), in the lungs and tissues of influenza virus-infected mice (52), and in  
148 mice infected with rhinovirus (53), and thus may represent a generalized cellular response to  
149 viral infection.

150 Lastly, the metabolites uridine tri-phosphate (UTP), UDP-glucose, and UDP-D-  
151 glucuronate were also increased in MNV-infected RAW cells (**Fig. 1C**). These metabolites are  
152 part of the glucuronic acid pathway that can lead to the generation of proteoglycans and other  
153 glycosylated forms of proteins (54) that have variable roles, including as potential extracellular  
154 signals (55, 56). Indeed, many hNoV strains, including the clinically relevant genogroup II,  
155 genotype 4 viruses, are able to bind to host extracellular glycans, i.e., histo-blood group antigens  
156 (57, 58). Collectively, our metabolomics survey suggests that macrophages respond to MNV  
157 infection by increasing: (i) the energy- and metabolite-generating pathways glycolysis and  
158 oxidative phosphorylation; (ii) adenosine catabolism, which may be a part of the general innate  
159 immune response; and, (iii) the glucuronic acid pathway, which may have effects on cellular  
160 protein glycosylation.



161

162 ***2DG reduces MNV-1 infection in RAW cells and bone marrow-derived macrophages.***

163 Metabolomics profiling of MNV infected RAW cells suggested that glycolysis and  
164 OXPHOS are increased during viral infection. But whether this increase creates an intracellular  
165 environment more supportive for viral replication, or rather represents an anti-viral immune  
166 strategy of the host cell, is unclear from such a survey. To test whether host cell glycolysis is  
167 supportive for effective MNV infection of macrophages in generating building blocks, viral  
168 infection was measured *in vitro* in the presence of the potent and commonly used glycolysis  
169 inhibitor 2-Deoxyglucose (2DG), a glucose analog that blocks early glycolysis (59, 60).

170 RAW cells were infected with MNV-1 at an MOI of five for one hour. Medium  
171 containing 10 mM 2DG was then added post-infection to exclude direct effects of the compound  
172 on virions. After an eight-hour incubation (one viral replication cycle), a greater than two log<sub>10</sub>  
173 decrease in the number of infectious viral particles in 2DG-treated cells was observed by plaque  
174 assay (**Fig. 2A**). RAW cells are a transformed cell line and generally engage in active “Warburg-  
175 effect” glycolysis (61). We therefore repeated the experiment in primary bone marrow-derived  
176 macrophages (BMDM) isolated from Balb/c mice to determine whether glycolysis is also  
177 relevant in non-transformed cells. 2DG treatment of BMDM caused an average one log<sub>10</sub>  
178 decrease in viral loads after eight hours (**Fig. 2B**). 2DG treatment did not inhibit RAW viability  
179 during an eight-hour treatment (**Fig. 2C**), but did reduce RAW cell viability by about 30% after  
180 24 hours (**Fig. S1A**).

181 Since RAW cells were grown in medium replete with glucose (~25 mM), putatively  
182 creating a competitive metabolic situation between glucose and 2DG, we next determined the  
183 minimal concentration of 2DG that significantly inhibited viral infection in RAW cells. Findings

184 from a dose-response study performed in the presence of glucose demonstrated that 2DG  
185 inhibited MNV-1 infection in a dose-dependent manner with the lowest significant inhibition at  
186 4.0 mM (**Fig. 2D**).

187 To determine the point during the infectious cycle that 2DG exerts its inhibitory effect on  
188 MNV, a time-of-addition study was performed. RAW cells were infected with MNV-1 and 2DG  
189 added to the medium at variable times post-infection. The results showed that 2DG had a  
190 significant effect on MNV infection when added to the culture up to two hours post-infection  
191 (**Fig. 2E**), suggesting that glycolysis is important for early steps in the viral life cycle.

192 These data are consistent with the notion that glycolysis is providing necessary building  
193 blocks for viral replication. Thus, to determine whether 2DG might be exerting a generalized  
194 anti-viral response in any transformed cell line against any virus, we tested viral infection of a  
195 different ssRNA virus, human astrovirus VA1, which is readily propagated in Caco-2 cells (62).  
196 Surprisingly, 2DG did not significantly inhibit human astrovirus infection *in vitro* (**Fig. 2F**),  
197 suggesting that the MNV phenotype in RAW cells and in BMDM is specific to MNV.

198 Taken together, these data demonstrate that host cell glycolysis, whether in primary or  
199 transformed cells, contributes to optimal MNV infection in macrophages. They further suggest  
200 that glycolysis is an intrinsic host factor that modulates infection in a virus-specific manner.

201

#### 202 ***2DG treatment inhibits MNV-1 (-) strand vRNA and viral non-structural protein production.***

203 Post-infection treatment of RAW cells with 2DG suggested that host cell glycolysis is  
204 important for early stages of MNV infection (**Fig. 2E**). To more accurately pinpoint the stage in  
205 the viral infectious cycle at which glycolysis is important, RAW cells were transfected directly  
206 with viral RNA (vRNA) in order to bypass the steps of binding, uptake and virion uncoating.

207 2DG treatment of transfected RAW cells resulted in about a two  $\log_{10}$  reduction of infectious  
208 virus particle production after 12 hours (**Fig. 3A**) and a one  $\log_{10}$  reduction at 24 hours (**Fig. S2**),  
209 suggesting that 2DG does not affect virion binding or genome uncoating of MNV.

210 MNV is a single-stranded, positive (+) strand, non-enveloped virus, and so the viral life-  
211 cycle involves uptake of viral particles, uncoating of the (+) strand vRNA, direct translation of  
212 the (+)-sense genome to produce the non-structural proteins (including the viral RNA  
213 polymerase), followed by viral negative (-) RNA strand synthesis for eventual production of new  
214 (+) strand vRNA, structural coat proteins, and progeny virion assembly (**Fig. 3B**). To measure  
215 vRNA production during 2DG treatment, we isolated RNA over the course of a 12-hour  
216 infection and assessed relative amounts of total and plus- and minus-strand vRNA (**Figs. 3C, D,**  
217 **and E**) (63). At four hours post-infection (hpi), no difference in the quantity of (+) strand and  
218 total vRNA was observed (**Figs. 3C and E**), indicating the same amount of virus infected the  
219 cells, confirming 2DG has no significant effect on viral binding and entry. However, there is a  
220 significant reduction in the amount of (-) strand vRNA at four hpi in 2DG-treated cells (**Fig. 3D**).  
221 At 8 and 12 hpi, there is significantly less vRNA overall for all species of RNA assessed (**Fig**  
222 **3C-E**). These data demonstrated although vRNA replication occurs in 2DG-treated cells, a lag  
223 occurred in transcription of (-) strand vRNA.

224 Since translation of the non-structural proteins precedes (-) strand vRNA synthesis, we  
225 next assessed the quantity of MNV non-structural protein using anti-ProPol/NS6&7 and anti-  
226 capsid antibodies by Western blot during 2DG treatment. Cells treated with 2DG contained no  
227 detectable Pol or VP1 proteins at 7 hpi, while reduced amounts of these proteins were present at  
228 12 hpi (**Fig. 3F**). These data indicate that host cell glycolysis is important for an early step in  
229 viral replication after delivery of the viral RNA into the cytosol.

230 Taken together, inhibition of glycolysis with 2DG did not affect the ability of RAW cells  
231 to internalize infectious virions, but it caused a delay in the translation of viral non-structural  
232 proteins and negative-strand RNA synthesis. It is currently unclear whether the decrease in (-)  
233 strand RNA levels are due to the reduced levels of viral non-structural proteins, including the  
234 viral polymerase, or a direct inhibitory effect of 2DG on vRNA synthesis.

235

### 236 *Inhibiting the pentose phosphate pathway reduces MNV infection of RAW cells*

237 The metabolomics survey outlined in Figure 1 demonstrated that the first metabolite  
238 produced from Glucose-6-phosphate in the oxidative half of the Pentose Phosphate Pathway  
239 (PPP), 6-phosphogluconate, was more abundant in MNV-infected cells. This suggested that the  
240 PPP, which branches off glycolysis at the early stage of glucose phosphorylation (64), may also  
241 be important for MNV infection in RAW cells. Also, since 2DG interferes at the level of glucose  
242 phosphorylation, the viral inhibition caused by 2DG may be due to interference with the PPP.

243 Therefore, to test the importance of the PPP for MNV infection, we used the inhibitor of  
244 the PPP enzyme glucose-6-dehydrogenase, 6-Aminonicotinamide (6AN). Treatment with 500  
245  $\mu$ M 6AN after MNV-1 infection caused a one  $\log_{10}$  reduction in the production of infectious  
246 MNV-1 after eight hours (**Fig. 4A**). 6AN was non-toxic to RAW cells up to 1.0 mM during eight  
247 hours (**Fig. 4B**), whereas all concentrations of 6AN tested caused an approximately 30%  
248 reduction in cell viability after 24 hours (**Fig. S1B**).

249 Inhibition of MNV infection by 2DG may be partially due to its effect on the PPP by  
250 depleting ribose nucleotides, one of the major end products of the PPP. Alphaviruses, which rely  
251 on host cell glycolysis via PI3 kinase signaling, are partially rescued for viral replication with  
252 ribose supplementation when PI3 kinase signaling is inhibited (65). Therefore, we infected RAW

253 cells with the minimal amount of 2DG that still causes a significant reduction in MNV infection  
254 (4 mM), and supplemented the cultures with ribose alone (**Fig. 4C**) or pre-supplemented cells  
255 with a mix of five ribonucleosides (**Fig. 4D**). Neither treatment was sufficient to increase viral  
256 titers during 2DG inhibition. These data suggest that, at least under the conditions tested, viral  
257 inhibition from 2DG is caused by cellular changes other than nucleotide availability.

258 ***2DG viral inhibition is independent of the type I interferon response.***

259 The mechanism of viral inhibition by 2DG could be due to a variety of cellular  
260 perturbations that are caused by a decrease in glycolysis. MNV infection in RAW cells induces a  
261 strong innate immune response, including interferon induction (66). Type I Interferons in turn  
262 are able to affect host cell metabolism (67, 68), and exhibit a strong anti-MNV response (69-71).  
263 Therefore, we determined whether 2DG inhibition of viral replication was dependent on type I  
264 interferon responses. Wild-type C57BL/6 BMDM and BMDM lacking the type I interferon  
265 receptor (IFNAR1<sup>-/-</sup>) were infected with MNV-1 for one hour and then treated cells with 10 mM  
266 2DG. After eight hours, both WT and IFNAR1<sup>-/-</sup> cells had reduced viral titers following 2DG  
267 treatment compared to untreated cells (**Fig. 5**). These data demonstrate that the inhibition of  
268 MNV infection by 2DG is independent of the antiviral type I interferon response.

269

270 ***MNV-1 infection increases activation of Akt but not AMPK $\alpha$***

271 To identify cellular signaling pathways that underlie the observed metabolic changes  
272 during MNV infection, we focused on two master regulators of metabolic control in cells, PI3-  
273 kinase/Akt and AMPK (72-80). In mammals, AMPK is able to sense the energetic status of cells,  
274 specifically the ratio of AMP and ADP relative to ATP, and can promote fatty acid oxidation and  
275 the expression of mitochondrial proteins (81-83). Western blot analysis of RAW cells revealed

276 very low levels of total AMPK $\alpha$  protein, and no increases in phosphorylation at Thr172 between  
277 mock- and virus-infected cells, or between untreated and 2DG-treated cells were observed (**Fig.**  
278 **6A and Fig. S3**). These data demonstrate that AMPK is not involved in the energetic changes in  
279 RAW cells that we have observed during MNV infection.

280 Another protein that has been implicated in energy sensing in multiple cell types is Akt.  
281 This kinase has been shown to play a key role in stimulating glycolysis and glucose metabolism  
282 via multiple mechanisms (72, 76, 84). In addition, Akt signaling is often altered during the  
283 infectious cycle of numerous viruses (85). Western blot analysis of Akt activation during MNV-1  
284 infection demonstrated that Akt phosphorylation at Ser473 was slightly elevated at 2 hpi (~2-  
285 fold) (**Fig. 6B and Fig. S3**) above the baseline level of Akt activation in mock-treated RAW  
286 cells. Akt was further activated as indicated by the higher level of Ser473 phosphorylation at 7  
287 hpi (~10-fold higher) (**Fig. 6B**) and 12 hpi (**Fig. S4**). 2DG treatment prevented these increases in  
288 Akt phosphorylation (**Fig. 6B**).

289 Because Akt phosphorylation was elevated during MNV infection and 2DG blocked Akt  
290 activation and viral replication, we asked whether inhibition of Akt signaling would inhibit MNV  
291 infection in RAW cells, linking Akt signaling with a change in host cell glycolysis. Treating cells  
292 with 15  $\mu$ M MK2206, a potent inhibitor of Akt phosphorylation, completely prevented Akt  
293 phosphorylation at Ser473 (**Fig. 6B**) but did not affect AMPK $\alpha$  phosphorylation (**Fig. 6A**).  
294 Treating RAW cells with 15  $\mu$ M MK2206 after the one hour MNV adsorption phase reduced  
295 viral production after eight hours by about one log<sub>10</sub> (**Fig. 6C**). Furthermore, 2DG and MK2206  
296 reduced RAW cell glycolysis irrespective of infection as measured by assaying end-point lactate  
297 production (**Fig. 6D**). Both compounds are non-toxic at these concentrations (**Fig. S1C and**  
298 **S1D**). These experiments demonstrate that Akt activation is a feature of MNV infection of RAW

299 cells, and that Akt plays a role in maintaining glycolysis in these cells. Akt activation during  
300 MNV infection is consistent with a previous transcriptomic study of monocytes transfected with  
301 the non-structural protein NS1-2, which implicated NS1-2 in affecting PI3K-Akt signaling  
302 pathways (86). Taken together, these data are consistent with a model whereby MNV infection  
303 upregulates glycolysis via Akt signaling.

304

## 305 **DISCUSSION**

306       When viruses infect cells, they are entirely dependent on the intracellular landscape of  
307 their hosts in order to replicate efficiently. Indeed the intracellular metabolic state of target cells  
308 acts as an intrinsic host factor, and a variety of metabolic pathways are important for successful  
309 viral infection (3). However, different viruses cause diverse metabolic effects in various cell  
310 types, and the mechanisms of viral engagement with host metabolic processes vary greatly (24-  
311 32). Thus, defining the specific host cell metabolic features that are required for individual  
312 viruses may reveal key host cell vulnerabilities that could be helpful for the future development  
313 of effective and safe antiviral therapies (46). Noroviruses lack effective therapies. In this study,  
314 we uncover central carbon metabolism as an intrinsic factor that is important for optimal  
315 infection of macrophages by MNV at early points during replication, suggesting a potential new  
316 anti-norovirus target.

317       Maintaining homeostasis of glucose metabolism in mammalian physiology is of  
318 importance in virtually every tissue, and glycolysis and OXPHOS are considered to be “central”  
319 carbon metabolism since they are a hub for multiple metabolic pathways, and their vital role in  
320 energy homeostasis. Therefore, it is not surprising that some viruses have evolved to take  
321 advantage of different aspects of these conserved pathways to their benefit. Interestingly,

322 glycolysis may be increased or decreased in response to viral infection, with similar beneficial  
323 outcomes for the virus. For instance, dengue virus increases both glucose uptake and  
324 transcription of the important enzyme hexokinase 2 (28), while herpes simplex type 1 activates  
325 glycolysis by increasing transcription and activation of the enzyme phosphofructokinase-1 (PFK-  
326 1) (33), with both viruses relying on active glycolysis for optimal infection. On the other hand,  
327 Kaposi's sarcoma-associated herpesvirus (KSHV) causes a suppression of both aerobic  
328 glycolysis and OXPHOS in transformed cells under nutrient stress, which thereby inhibits cell  
329 death and enhances viral survival in this model of the tumor microenvironment (24). Our  
330 observation that astrovirus infection was not affected by the treatment of Caco-2 cells with 2DG  
331 highlights that not all viruses require glycolysis in transformed cells, which generally conduct a  
332 significant level of "Warburg Effect" glycolysis at baseline (61). Thus, it was notable that 2DG  
333 inhibited MNV infection in non-transformed primary cells, highlighting the fact that carbon  
334 metabolism has pro-viral functions during norovirus infection. These results illustrate that the  
335 relationship of target cell metabolism to viral infection is cell type-specific and virus-specific.

336 Another notable aspect of the relationship between carbon metabolism and infection is  
337 the finding that glycolysis may facilitate infection outside of a canonical, metabolic role. HIV-1  
338 causes an increase in expression of hexokinase-1 (HK1) accompanied by a decrease in enzymatic  
339 activity (87). Our findings with 2DG, which targets the enzymatic activity of hexokinase, points  
340 to a metabolic, rather than non-metabolic, role for glycolysis during norovirus infection.  
341 Specifically, glucose-6-phosphate (G6P), located at the intersection of glycolysis and PPP, is a  
342 major hub for macrophage metabolic regulation of MNV infection given that inhibition of the  
343 PPP also reduced viral infection.



344           One particular caveat of host cell metabolic profiling studies is the complexity of  
345 metabolic responses that immune cells can adopt in response to various stimuli. This is of  
346 particular relevance for macrophages. Although the M0/M1/M2 system of categorizing  
347 macrophage metabolic states is a useful construct for generalizing inflammatory versus non-  
348 inflammatory activity, these cells establish a complex range of metabolic phenotypes (22, 88,  
349 89). For example, although the bacterial product LPS causes an increase in glycolysis and a  
350 decrease in OXPHOS in human monocytes, a different bacterial product, Pam3CysSK4 (P3C),  
351 causes both pathways to increase (23). Thus, two different bacterial products signaling through  
352 different Toll-like receptors (TLRs) establish unique metabolic profiles. This finding emphasizes  
353 that unique pathogens elicit complex host metabolic responses, and that the range of molecular  
354 signals that immune cells are responding to *in vivo* may determine the susceptibility of cell types  
355 to certain infections. The metabolomics survey in this study demonstrated that MNV infection,  
356 like P3C treatment, elicits an increase in both glycolysis and OXPHOS, and ongoing work is  
357 seeking to reveal the individual contributions of these two pathways to norovirus infection. In  
358 addition, since macrophages are target cells of MNV *in vivo* (44, 90), it is conceivable that their  
359 metabolic status during infection influences the establishment of norovirus infection at the  
360 cellular levels with potential influences on viral pathogenesis. However, future studies are  
361 needed to test this.

362           Another important aspect of macrophage metabolism is how metabolic rewiring controls  
363 functional outputs, such as microbial killing mechanisms and cytokine/chemokine production  
364 (7), which in turn could indirectly affect viral infection. Akt has been implicated in regulating  
365 reactive oxygen species (ROS) generation (75). Although MNV infection increased Akt  
366 activation, we did not observe an increase in general ROS in RAW cells upon 2DG treatment

367 **(Fig. S5)**. Furthermore, blocking glycolysis with 2DG did not cause a significant difference in  
368 the production of the inflammatory cytokine TNF $\alpha$  in 2DG-treated RAW cells during MNV  
369 infection **(Fig. S6)**. Combined with the finding that the effect of 2DG is independent of type I  
370 IFN signaling, these data suggest that the antiviral effect of 2DG is not mediated via immune  
371 signaling. However, whether MNV affects general macrophage functions via Akt activation and  
372 metabolic rewiring of these cells will need to be tested in future studies.

373 A general caveat to the use of pharmacologic inhibitors in biological systems is their  
374 potential for inducing side effects. Although 2DG has been commonly used as a prototypical  
375 glycolysis inhibitor (59, 60), it may also affect other aspects of cell behavior that can influence  
376 infectivity. For example, 2DG has been shown to induce ROS-triggered autophagy via AMPK  
377 (91). This pathway is unlikely to be involved in the antiviral activity of 2DG in our studies  
378 considering the lack of ROS induction upon 2DG treatment in RAW cells **(Fig. S5)**, and the lack  
379 of AMPK induction during infection. Another study showed that 2DG can be damaging for  
380 certain viral infections via initiation of an ER stress response in mice (92). Similarly, 2DG  
381 decreases porcine epidemic diarrhea virus infection *in vitro* via triggering the unfolded protein  
382 response and reducing protein translation (93). Our work showed that 2DG inhibited MNV  
383 infection early during the viral life cycle, affecting the translation of non-structural proteins and  
384 the transcription of new viral genomes. However, the virus does eventually begin to replicate  
385 genomes and produce viral proteins even in the presence of 2DG. Thus, the mechanism by which  
386 2DG causes this lag in the MNV life cycle could be via a rapid cellular stress response, or a  
387 decrease in specific metabolites, or a combination of the two, and additional studies are needed  
388 to clarify the relative contribution of both.

389           Lastly, it should be noted that a variety of metabolites, including Ornithine, 3-Phospho-  
390 Serine, Creatinine among others, were also increased during MNV infection. While these  
391 molecules could be important host factors for viral infection, they were not explored further here.  
392 Such investigations and an extension of metabolic findings to human noroviruses are planned for  
393 the future. Human norovirus has remained stubbornly intractable to robust cultivation *in vitro*.  
394 Although there has been some success in infecting transformed B cells (40) and human intestinal  
395 enteroids (94) with human norovirus, viral loads remain low and an infectious, passagable cell  
396 culture-derived virus stock remains elusive (95). Identifying host cell factors such as metabolites  
397 and specific metabolic activities may therefore aid in optimizing *in vitro* cultivation systems for  
398 human noroviruses.

399           In conclusion, we have shown that central carbon metabolism in macrophages is an  
400 intrinsic factor promoting optimal infection of a norovirus. Our data are consistent with a model  
401 whereby MNV activates the protein kinase Akt to increase central carbon metabolism in  
402 macrophages. The glycolysis inhibitor 2DG inhibits norovirus (but not astrovirus) infection,  
403 independent of the type I IFN response by limiting non-structural protein translation and viral  
404 RNA synthesis. These findings reveal cellular metabolism as a potential therapeutic target for  
405 norovirus and suggest a new strategy for improving human norovirus culture systems.

406 **MATERIALS AND METHODS**

407 Detailed methods can be found in Text S1 in the supplemental material.

408 **Compounds and reagents:** Please refer to Text S1 in the supplemental material for details.

409 **Cell culture and virus strains:** RAW 264.7 and Caco-2 cells were obtained from ATCC. The  
410 plaque purified MNV-1 clone (GV/MNV1/2002/USA) MNV-1.CW3 (43) (referred herein as  
411 MNV-1) was used at passage 6 in all experiments.

412 **Virus infections, virus transfection, and plaque assay:** All MNV infections were done in the  
413 RAW 264.7 cell line, Balb/c primary bone marrow-derived macrophages (BMDM from male  
414 mice) or BMDM from WT and IFNAR1-knockout cells on a C57Bl6 background. Transfections  
415 and viral enumerations were performed similar to (62, 96, 97). Please refer to supplemental  
416 material for details.

417 **Cell viability assay:** Cell viability was tested using Resazurin reagent according to the  
418 manufacturer's recommendations (Biotium 30025-1).

419 **RNA extraction and RT-qPCR:** Experiments were performed per manufacturer's directions  
420 using Chloroform extraction (Trizol) or the Zymo Research Direct-zol RNA MiniPrep Plus  
421 (R2072).

422 **Strand-specific RT-qPCR:** Strand-specific RT-qPCR for MNV was performed as previously  
423 described (63).

424 **Protein extraction, SDS-PAGE and immunoblotting:** Experimental conditions and antibodies  
425 are detailed in supplemental material.

426 **Metabolomics assay:** Samples were analyzed at the Michigan Regional Comprehensive  
427 Metabolomics Resource Core (MRC<sup>2</sup>) at the University of Michigan by Mass Spectrometry as  
428 detailed in supplemental material.

429 **Lactate assay:** Cell supernatants were assessed for lactate using the Cayman Chemical  
430 Glycolysis Cell-Based Assay Kit (600450) per the manufacturer's protocol.  
431 **ELISA:** Cytokine levels were determined at the University of Michigan Rogel Cancer Center  
432 Immunological Monitoring Core by ELISA (Duosets, R&D Systems, Minneapolis, MN) as  
433 detailed in supplemental materials.  
434 **Statistical Analysis:** Metabolomics data were analyzed in Metaboanalyst 4.0. For all other  
435 experiments, data were analyzed in Prism7 using tests as indicated in Figure legends.

436

#### 437 **ACKNOWLEDGMENTS**

438 This work was in part supported by NIH/NIAID R21/R33 AI102106 to C.E.W. and M.O.R. and  
439 the University of Michigan BMRC Bridging Support program. J.L. and I.G. are supported by  
440 grants from the Wellcome Trust (Ref: 207498/Z/17/Z) and the UK Biotechnology and Biological  
441 Sciences Research Council (Ref: BB/N001176/1). The work on this manuscript utilized  
442 Metabolomics Core Services supported by grant U24 DK097153 of NIH Common Funds Project  
443 to the University of Michigan. We thank Dr. Kim Green (NIH, NIAID, USA) for the ProPol  
444 antibody, Dr. Megan Baldrige (Washington University in St. Louis, MO, USA) for IFNAR-/-  
445 bone marrow, and the members of the O'Riordan and Wobus laboratories for suggestions.

446

#### 447 **AUTHOR CONTRIBUTIONS**

448 KDP, AOK, MXDOR, CEW conceived the experiments. KDP, AOK, JL, JRA, RJM carried out  
449 the experiments. KDP, AOK, JL analyzed the data. KDP, AOK, IG, MXDOR, CEW contributed  
450 to the interpretation of the results. KDP and CEW wrote the manuscript in consultation with IG  
451 and MXDOR.

452 **FIGURE LEGENDS**

453 **Fig 1. Metabolomics survey of RAW 264.7 cells infected with MNV-1 reveal several**  
454 **metabolic pathways that are increased during infection.**

455 (A) Measurements of select metabolites from central carbon metabolism, including glycolysis,  
456 the Pentose Phosphate Pathway (PPP), and the Tricarboxylic Acid Cycle (TCA). (B) Metabolites  
457 from Xanthine biosynthesis (Purine metabolism), and (C) the UDP-Glucuronate pathway  
458 (Glucuronic acid pathway). Schematics of the metabolic pathways shown are simplified for  
459 clarity. All metabolites assayed are listed in Tables 1 and 2 with mean and standard deviation for  
460 three MNV-1 infected samples (MOI = 5) and four mock-infected samples (mock cell lysate).  
461 Infection was 8 hours. ♦Indicates where in the pathway UTP is consumed. Analyses performed  
462 in Metaboanalyst using student's t-test. \* $P < 0.05$ ; \*\* $P < 0.01$ ; ns = not significant.

463

464 **Fig 2. Effects of 2-Deoxyglucose (2DG) on MNV-1 and human astrovirus VA1 infection *in***  
465 ***vitro*.**

466 (A) 2DG (10 mM) reduces MNV-1 infection in RAW cells ( $\sim 2 \log_{10}$ ), and (B) primary Bone-  
467 marrow derived macrophages ( $\sim 1 \log_{10}$ ) (BMDM-Balb/C mice). 8-hour infections with MOI=5.  
468 (C) Cell viability assay (Resazurin reagent) showing that 2DG does not reduce RAW cell  
469 viability during 8-hours of exposure. Cell viability at 24 hours in Figure S1A. (D) Effects of  
470 different concentrations of 2DG on MNV-1 infection in RAW cells. (E) MNV-1 infection in  
471 RAW cells with 2DG added at different times post-infection. (F) 2DG does not affect infection  
472 of human astrovirus VA1 in Caco-2 cells (2DG 10 mM; 2CMC positive control 50  $\mu$ M).  
473 Toxicity of 2DG on Caco-2 cells in Fig S1E. (A, B, D and E) measured by Plaque Assay.  
474 Astrovirus in (F) was measured by RT-qPCR of viral RNA. Mann-Whitney test used for (A, B,

475 F) where \*\*\*\* $P < 0.0001$ . Kruskal-Wallis test with Dunn's multiple comparisons test used for (E)  
476 where \*\*\*\* $P < 0.0001$  and ns = not significant. Experiments represent combined data from at  
477 least three independent experiments except (F), which represents two experiments.

478

479 **Fig 3. 2DG treatment inhibits MNV infection early after viral uptake and uncoating.**

480 (A) MNV-1 viral RNA (vRNA) was transfected into RAW cells and then treated with 10 mM  
481 2DG. Data are from two independent experiments. (B) A simplified overview of the events in the  
482 MNV-1 life cycle. Callouts indicate points of the viral life cycle that may be affected during  
483 2DG treatment. (C & D) Strand-specific RT-qPCR of (C) plus (+) and (D) minus (-) MNV  
484 vRNA strands from RAW cells infected with MNV-1 for 4, 8 and 12 hours with and without  
485 2DG treatment (10 mM). (E) Taq-Man RT-qPCR of total MNV-1 viral RNA (non-strand  
486 specific) from the same RNA samples used for (C) and (D). Data are combined from three  
487 independent experiments with three replicates per experiment. (F) Western blot analysis of non-  
488 structural (Pol) and structural (Capsid) viral proteins after 7 and 12-hour infection of RAW cells  
489 in untreated and 2DG treated cells.  $\beta$ -Actin was used as a loading control for overall protein  
490 loading content. Solid line indicates 50 kDa ladder. Data shown are a representative Western  
491 blots from two independent experiments. Numbers below blots indicate densitometry  
492 measurement of protein in 2DG relative to untreated cells at 12 hours (average of two  
493 experiments). Mock-infected cells served as negative control. Mann-Whitney test used for (A)  
494 where \*\*\*\* $P < 0.0001$ . Two-way ANOVA with Dunnett's multiple comparisons test used for (C,  
495 D and E) where \*\* $P < 0.01$ ; \*\*\*\* $P < 0.0001$ ; ns = not significant. PFU=plaque forming units.

496

497 **Fig 4. The pentose phosphate pathway makes a minor contribution to MNV infection of**  
498 **RAW cells.**

499 (A) 6-Aminonicotinamide (6AN) (500  $\mu$ M), the inhibitor of 6-phosphogluconate dehydrogenase,  
500 reduces MNV infection in RAW cells (MOI = 5). (B) Resazurin cell viability assay of RAW  
501 cells treated with indicated concentration of 6AN for 8 hours (see S1B for 24h). (C)  
502 Supplementing MNV-infected RAW cells with 50 mM Ribose or (D) 50  $\mu$ M nucleosides (ncs)  
503 does not alleviate the viral growth inhibition caused by 4.5 or 4.0 mM 2DG treatment after 8-  
504 hour infection. Nucleosides (ncs) used in (D) were 50  $\mu$ M each of adenosine, guanosine,  
505 thymidine, cytidine, and uridine. RAW cells were treated overnight before infection with  
506 nucleosides, and again supplemented with nucleosides after infection with MNV. Mann-Whitney  
507 test in (A). Kruskal-Wallis test with Dunn's multiple comparisons test in (C) and (D).  
508 \*\*\*\* $P < 0.0001$ ; ns = not significant. PFU=Plaque Forming Units. DMSO is vehicle control used  
509 in v/v match to 6AN or ncs treatment. Data represent combination of three independent  
510 experiments.

511

512 **Fig 5. 2DG inhibition of MNV infection is independent of the Type I interferon response.**

513 2DG treatment reduces MNV infection in both WT BMDM and in BMDM lacking the Type I  
514 Interferon Receptor (IFNAR1 Knockout Cells) (WT-2DG versus IFNAR-2DG). Kruskal-Wallis  
515 test with Dunn's multiple comparisons post-test. \*\*\*\* $P < 0.0001$ ; ns = not significant. Data  
516 represent a combination of three independent experiments.

517

518 **Fig 6. MNV upregulates glycolysis via Akt signaling.**



519 (A-B) Western blot analysis of RAW cells infected with MNV (MOI=5) for 2 and 7-hours for  
520 (A) AMPK $\alpha$  and phospho-AMPK $\alpha$  (Thr172), and (B) Akt and phospho-Akt (Ser473).  
521 Treatments were 10 mM 2DG and 15  $\mu$ M MK2206. Western blot from 12hpi in FigS3.  $\beta$ -actin  
522 was used as loading control and for densitometry normalization. Graphs on the left represent  
523 densitometry analysis comparing protein phospho-protein relative to mock-infected cells at 7hpi.  
524 Graphs of densitometry analysis for 2hpi are in FigS4. (C) Inhibition of Akt phosphorylation  
525 with MK2206 reduces MNV-1 infection of RAW cells by about 0.75 log<sub>10</sub>. (D) Measurement of  
526 glycolysis via lactate production in mock and MNV-infected RAW cells after an 8-hour infection  
527 (MOI=5). Cells were treated with 10 mM 2DG and 15  $\mu$ M MK2206. Mann-Whitney test used in  
528 (C) where \*\*\*\* $P$ <0.0001 (combined three independent experiments). One-Way ANOVA used in  
529 (D) with Dunnett's multiple comparisons test (graph shows data for one of two independent  
530 experiments with three replicates each).  
531  
532

## 533 REFERENCES

- 534 1. Sanchez EL, Lagunoff M. 2015. Viral activation of cellular metabolism. *Virology* 479-  
535 480:609-18.
- 536 2. Freyberg Z, Harvill ET. 2017. Pathogen manipulation of host metabolism: A common  
537 strategy for immune evasion. *PLoS Pathog* 13:e1006669.
- 538 3. Goodwin CM, Xu S, Munger J. 2015. Stealing the Keys to the Kitchen: Viral  
539 Manipulation of the Host Cell Metabolic Network. *Trends Microbiol* 23:789-798.
- 540 4. O'Neill LA, Kishton RJ, Rathmell J. 2016. A guide to immunometabolism for  
541 immunologists. *Nat Rev Immunol* 16:553-65.
- 542 5. Buchakjian MR, Kornbluth S. 2010. The engine driving the ship: metabolic steering of  
543 cell proliferation and death. *Nat Rev Mol Cell Biol* 11:715-27.
- 544 6. Olenchock BA, Rathmell JC, Vander Heiden MG. 2017. Biochemical Underpinnings of  
545 Immune Cell Metabolic Phenotypes. *Immunity* 46:703-713.
- 546 7. O'Neill LA, Pearce EJ. 2016. Immunometabolism governs dendritic cell and macrophage  
547 function. *J Exp Med* 213:15-23.
- 548 8. Kaur J, Debnath J. 2015. Autophagy at the crossroads of catabolism and anabolism. *Nat*  
549 *Rev Mol Cell Biol* 16:461-72.
- 550 9. Galluzzi L, Pietrocola F, Levine B, Kroemer G. 2014. Metabolic control of autophagy.  
551 *Cell* 159:1263-76.
- 552 10. Olive AJ, Sassetti CM. 2016. Metabolic crosstalk between host and pathogen: sensing,  
553 adapting and competing. *Nat Rev Microbiol* 14:221-34.
- 554 11. Caradonna KL, Engel JC, Jacobi D, Lee CH, Burleigh BA. 2013. Host metabolism  
555 regulates intracellular growth of *Trypanosoma cruzi*. *Cell Host Microbe* 13:108-17.
- 556 12. Bravo-Santano N, Ellis JK, Mateos LM, Calle Y, Keun HC, Behrends V, Letek M. 2018.  
557 Intracellular *Staphylococcus aureus* Modulates Host Central Carbon Metabolism To  
558 Activate Autophagy. *mSphere* 3.
- 559 13. Eisenreich W, Heesemann J, Rudel T, Goebel W. 2015. Metabolic Adaptations of  
560 Intracellular Bacterial Pathogens and their Mammalian Host Cells during Infection  
561 ("Pathometabolism"). *Microbiol Spectr* 3.
- 562 14. Hu Z, Zou Q, Su B. 2018. Regulation of T cell immunity by cellular metabolism. *Front*  
563 *Med* doi:10.1007/s11684-018-0668-2.
- 564 15. Na YR, Gu GJ, Jung D, Kim YW, Na J, Woo JS, Cho JY, Youn H, Seok SH. 2016. GM-  
565 CSF Induces Inflammatory Macrophages by Regulating Glycolysis and Lipid  
566 Metabolism. *J Immunol* 197:4101-4109.
- 567 16. McGettrick AF, O'Neill LA. 2013. How metabolism generates signals during innate  
568 immunity and inflammation. *J Biol Chem* 288:22893-8.
- 569 17. Loftus RM, Finlay DK. 2016. Immunometabolism: Cellular Metabolism Turns Immune  
570 Regulator. *J Biol Chem* 291:1-10.
- 571 18. Lee YS, Wollam J, Olefsky JM. 2018. An Integrated View of Immunometabolism. *Cell*  
572 172:22-40.
- 573 19. Norata GD, Caligiuri G, Chavakis T, Matarese G, Netea MG, Nicoletti A, O'Neill LA,  
574 Marelli-Berg FM. 2015. The Cellular and Molecular Basis of Translational  
575 Immunometabolism. *Immunity* 43:421-34.
- 576 20. Hotamisligil GS. 2017. Foundations of Immunometabolism and Implications for  
577 Metabolic Health and Disease. *Immunity* 47:406-420.

- 578 21. Biswas SK, Mantovani A. 2012. Orchestration of metabolism by macrophages. *Cell*  
579 *Metab* 15:432-7.
- 580 22. Mosser DM, Edwards JP. 2008. Exploring the full spectrum of macrophage activation.  
581 *Nat Rev Immunol* 8:958-69.
- 582 23. Lachmandas E, Boutens L, Ratter JM, Hijmans A, Hooiveld GJ, Joosten LA, Rodenburg  
583 RJ, Franssen JA, Houtkooper RH, van Crevel R, Netea MG, Stienstra R. 2016. Microbial  
584 stimulation of different Toll-like receptor signalling pathways induces diverse metabolic  
585 programmes in human monocytes. *Nat Microbiol* 2:16246.
- 586 24. Zhu Y, Ramos da Silva S, He M, Liang Q, Lu C, Feng P, Jung JU, Gao SJ. 2016. An  
587 Oncogenic Virus Promotes Cell Survival and Cellular Transformation by Suppressing  
588 Glycolysis. *PLoS Pathog* 12:e1005648.
- 589 25. Barrero CA, Datta PK, Sen S, Deshmane S, Amini S, Khalili K, Merali S. 2013. HIV-1  
590 Vpr modulates macrophage metabolic pathways: a SILAC-based quantitative analysis.  
591 *PLoS One* 8:e68376.
- 592 26. Bilz NC, Jahn K, Lorenz M, Ludtke A, Hubschen JM, Geyer H, Mankertz A, Hubner D,  
593 Liebert UG, Claus C. 2018. Rubella Viruses Shift Cellular Bioenergetics to a More  
594 Oxidative and Glycolytic Phenotype with a Strain-Specific Requirement for Glutamine. *J*  
595 *Virol* 92.
- 596 27. Chen IT, Lee DY, Huang YT, Kou GH, Wang HC, Chang GD, Lo CF. 2016. Six Hours  
597 after Infection, the Metabolic Changes Induced by WSSV Neutralize the Host's Oxidative  
598 Stress Defenses. *Sci Rep* 6:27732.
- 599 28. Fontaine KA, Sanchez EL, Camarda R, Lagunoff M. 2015. Dengue virus induces and  
600 requires glycolysis for optimal replication. *J Virol* 89:2358-66.
- 601 29. Gualdoni GA, Mayer KA, Kapsch AM, Kreuzberg K, Puck A, Kienzl P, Oberndorfer F,  
602 Fruhwirth K, Winkler S, Blaas D, Zlabinger GJ, Stockl J. 2018. Rhinovirus induces an  
603 anabolic reprogramming in host cell metabolism essential for viral replication. *Proc Natl*  
604 *Acad Sci U S A* doi:10.1073/pnas.1800525115.
- 605 30. Ripoli M, D'Aprile A, Quarato G, Sarasin-Filipowicz M, Gouttenoire J, Scrima R, Cela  
606 O, Boffoli D, Heim MH, Moradpour D, Capitanio N, Piccoli C. 2010. Hepatitis C virus-  
607 linked mitochondrial dysfunction promotes hypoxia-inducible factor 1 alpha-mediated  
608 glycolytic adaptation. *J Virol* 84:647-60.
- 609 31. Smallwood HS, Duan S, Morfouace M, Rezinciuc S, Shulkin BL, Shelat A, Zink EE,  
610 Milasta S, Bajracharya R, Oluwaseun AJ, Roussel MF, Green DR, Pasa-Tolic L, Thomas  
611 PG. 2017. Targeting Metabolic Reprogramming by Influenza Infection for Therapeutic  
612 Intervention. *Cell Rep* 19:1640-1653.
- 613 32. Thai M, Graham NA, Braas D, Nehil M, Komisopoulou E, Kurdistani SK, McCormick F,  
614 Graeber TG, Christofk HR. 2014. Adenovirus E4ORF1-induced MYC activation  
615 promotes host cell anabolic glucose metabolism and virus replication. *Cell Metab* 19:694-  
616 701.
- 617 33. Abrantes JL, Alves CM, Costa J, Almeida FC, Sola-Penna M, Fontes CF, Souza TM.  
618 2012. Herpes simplex type 1 activates glycolysis through engagement of the enzyme 6-  
619 phosphofructo-1-kinase (PFK-1). *Biochim Biophys Acta* 1822:1198-206.
- 620 34. Glass RI, Parashar UD, Estes MK. 2009. Norovirus gastroenteritis. *N Engl J Med*  
621 361:1776-85.

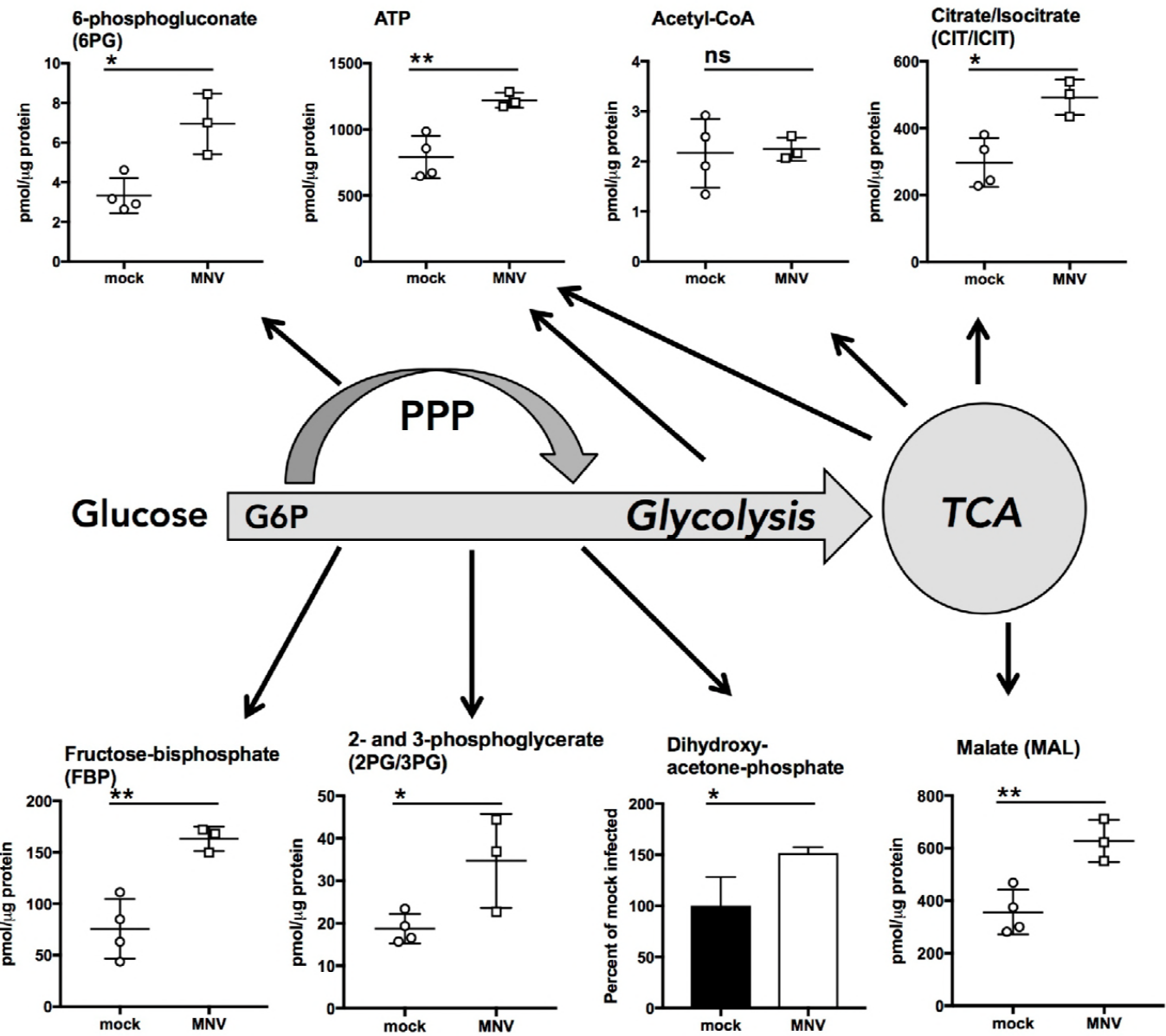
- 622 35. Ahmed SM, Hall AJ, Robinson AE, Verhoef L, Premkumar P, Parashar UD, Koopmans  
623 M, Lopman BA. 2014. Global prevalence of norovirus in cases of gastroenteritis: a  
624 systematic review and meta-analysis. *Lancet Infect Dis* 14:725-730.
- 625 36. Bartsch SM, Lopman BA, Ozawa S, Hall AJ, Lee BY. 2016. Global Economic Burden of  
626 Norovirus Gastroenteritis. *PLoS One* 11:e0151219.
- 627 37. Lopman BA, Steele D, Kirkwood CD, Parashar UD. 2016. The Vast and Varied Global  
628 Burden of Norovirus: Prospects for Prevention and Control. *PLoS Med* 13:e1001999.
- 629 38. Chang KO, Sosnovtsev SV, Belliot G, King AD, Green KY. 2006. Stable expression of a  
630 Norwalk virus RNA replicon in a human hepatoma cell line. *Virology* 353:463-73.
- 631 39. Duizer E, Schwab KJ, Neill FH, Atmar RL, Koopmans MP, Estes MK. 2004. Laboratory  
632 efforts to cultivate noroviruses. *J Gen Virol* 85:79-87.
- 633 40. Jones MK, Grau KR, Costantini V, Kolawole AO, de Graaf M, Freiden P, Graves CL,  
634 Koopmans M, Wallet SM, Tibbetts SA, Schultz-Cherry S, Wobus CE, Vinje J, Karst SM.  
635 2015. Human norovirus culture in B cells. *Nat Protoc* 10:1939-47.
- 636 41. Kolawole AO, Rocha-Pereira J, Elftman MD, Neyts J, Wobus CE. 2016. Inhibition of  
637 human norovirus by a viral polymerase inhibitor in the B cell culture system and in the  
638 mouse model. *Antiviral Res* 132:46-9.
- 639 42. Costantini V, Morantz EK, Browne H, Ettayebi K, Zeng XL, Atmar RL, Estes MK, Vinje  
640 J. 2018. Human Norovirus Replication in Human Intestinal Enteroids as Model to  
641 Evaluate Virus Inactivation. *Emerg Infect Dis* 24:1453-1464.
- 642 43. Thackray LB, Wobus CE, Chachu KA, Liu B, Alegre ER, Henderson KS, Kelley ST,  
643 Virgin HWt. 2007. Murine noroviruses comprising a single genogroup exhibit biological  
644 diversity despite limited sequence divergence. *J Virol* 81:10460-73.
- 645 44. Wobus CE, Karst SM, Thackray LB, Chang KO, Sosnovtsev SV, Belliot G, Krug A,  
646 Mackenzie JM, Green KY, Virgin HW. 2004. Replication of Norovirus in cell culture  
647 reveals a tropism for dendritic cells and macrophages. *PLoS Biol* 2:e432.
- 648 45. Wobus CE, Thackray LB, Virgin HWt. 2006. Murine norovirus: a model system to study  
649 norovirus biology and pathogenesis. *J Virol* 80:5104-12.
- 650 46. Ikeda M, Kato N. 2007. Modulation of host metabolism as a target of new antivirals. *Adv*  
651 *Drug Deliv Rev* 59:1277-89.
- 652 47. Wobus CE. 2018. The Dual Tropism of Noroviruses. *J Virol* 92.
- 653 48. Zhu L, Zhao Q, Yang T, Ding W, Zhao Y. 2015. Cellular metabolism and macrophage  
654 functional polarization. *Int Rev Immunol* 34:82-100.
- 655 49. Chen H, Yang T, Zhu L, Zhao Y. 2015. Cellular metabolism on T-cell development and  
656 function. *Int Rev Immunol* 34:19-33.
- 657 50. Perry JW, Taube S, Wobus CE. 2009. Murine norovirus-1 entry into permissive  
658 macrophages and dendritic cells is pH-independent. *Virus Res* 143:125-9.
- 659 51. Ziegler DW, Hutchinson HD, Kissling RE. 1971. Induction of xanthine oxidase by virus  
660 infections in newborn mice. *Infect Immun* 3:237-42.
- 661 52. Akaike T, Ando M, Oda T, Doi T, Ijiri S, Araki S, Maeda H. 1990. Dependence on O2-  
662 generation by xanthine oxidase of pathogenesis of influenza virus infection in mice. *J*  
663 *Clin Invest* 85:739-45.
- 664 53. Papi A, Contoli M, Gasparini P, Bristot L, Edwards MR, Chicca M, Leis M, Ciaccia A,  
665 Caramori G, Johnston SL, Pinamonti S. 2008. Role of xanthine oxidase activation and  
666 reduced glutathione depletion in rhinovirus induction of inflammation in respiratory  
667 epithelial cells. *J Biol Chem* 283:28595-606.

- 668 54. Lander AD, Selleck SB. 2000. The elusive functions of proteoglycans: in vivo veritas. *J*  
669 *Cell Biol* 148:227-32.
- 670 55. Lazarowski ER, Boucher RC. 2001. UTP as an extracellular signaling molecule. *News*  
671 *Physiol Sci* 16:1-5.
- 672 56. Lazarowski ER, Shea DA, Boucher RC, Harden TK. 2003. Release of cellular UDP-  
673 glucose as a potential extracellular signaling molecule. *Mol Pharmacol* 63:1190-7.
- 674 57. Schrotten H, Hanisch FG, Hansman GS. 2016. Human Norovirus Interactions with Histo-  
675 Blood Group Antigens and Human Milk Oligosaccharides. *J Virol* 90:5855-5859.
- 676 58. Marionneau S, Ruvoen N, Le Moullac-Vaidye B, Clement M, Cailleau-Thomas A, Ruiz-  
677 Palacois G, Huang P, Jiang X, Le Pendu J. 2002. Norwalk virus binds to histo-blood  
678 group antigens present on gastroduodenal epithelial cells of secretor individuals.  
679 *Gastroenterology* 122:1967-77.
- 680 59. Wick AN, Drury DR, Nakada HI, Wolfe JB. 1957. Localization of the primary metabolic  
681 block produced by 2-deoxyglucose. *J Biol Chem* 224:963-9.
- 682 60. Barban S, Schulze HO. 1961. The effects of 2-deoxyglucose on the growth and  
683 metabolism of cultured human cells. *J Biol Chem* 236:1887-90.
- 684 61. Vander Heiden MG, Cantley LC, Thompson CB. 2009. Understanding the Warburg  
685 effect: the metabolic requirements of cell proliferation. *Science* 324:1029-33.
- 686 62. Janowski AB, Bauer IK, Holtz LR, Wang D. 2017. Propagation of astrovirus VA1, a  
687 neurotropic human astrovirus, in cell culture. *J Virol* doi:10.1128/JVI.00740-17.
- 688 63. Vashist S, Urena L, Goodfellow I. 2012. Development of a strand specific real-time RT-  
689 qPCR assay for the detection and quantitation of murine norovirus RNA. *J Virol Methods*  
690 184:69-76.
- 691 64. Stincone A, Prigione A, Cramer T, Wamelink MM, Campbell K, Cheung E, Olin-  
692 Sandoval V, Gruning NM, Kruger A, Tauqeer Alam M, Keller MA, Breitenbach M,  
693 Brindle KM, Rabinowitz JD, Ralser M. 2015. The return of metabolism: biochemistry  
694 and physiology of the pentose phosphate pathway. *Biol Rev Camb Philos Soc* 90:927-63.
- 695 65. Mazon M, Castro C, Thaa B, Liu L, Mutso M, Liu X, Mahalingam S, Griffin JL, Marsh  
696 M, McInerney GM. 2018. Alphavirus-induced hyperactivation of PI3K/AKT directs pro-  
697 viral metabolic changes. *PLoS Pathog* 14:e1006835.
- 698 66. Enosi Tuipulotu D, Netzler NE, Lun JH, Mackenzie JM, White PA. 2017. RNA  
699 Sequencing of Murine Norovirus-Infected Cells Reveals Transcriptional Alteration of  
700 Genes Important to Viral Recognition and Antigen Presentation. *Front Immunol* 8:959.
- 701 67. Fritsch SD, Weichhart T. 2016. Effects of Interferons and Viruses on Metabolism. *Front*  
702 *Immunol* 7:630.
- 703 68. Raniga K, Liang C. 2018. Interferons: Reprogramming the Metabolic Network against  
704 Viral Infection. *Viruses* 10.
- 705 69. Changotra H, Jia Y, Moore TN, Liu G, Kahan SM, Sosnovtsev SV, Karst SM. 2009.  
706 Type I and type II interferons inhibit the translation of murine norovirus proteins. *J Virol*  
707 83:5683-92.
- 708 70. Thackray LB, Duan E, Lazear HM, Kambal A, Schreiber RD, Diamond MS, Virgin HW.  
709 2012. Critical role for interferon regulatory factor 3 (IRF-3) and IRF-7 in type I  
710 interferon-mediated control of murine norovirus replication. *J Virol* 86:13515-23.
- 711 71. Ng YC, Kim YW, Lee JS, Lee SJ, Jung Song M. 2018. Antiviral activity of *Schizonepeta*  
712 *tenuifolia* Briquet against noroviruses via induction of antiviral interferons. *J Microbiol*  
713 56:683-689.

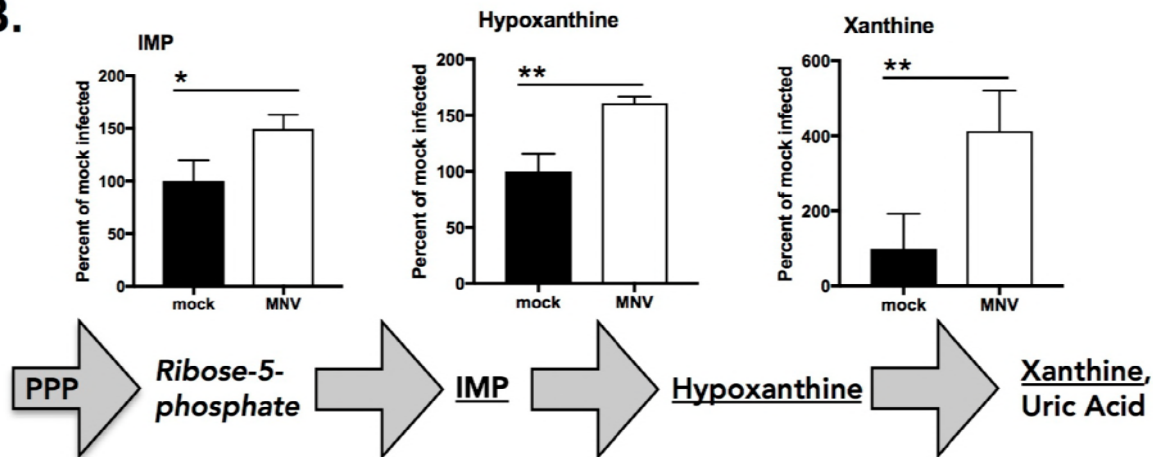
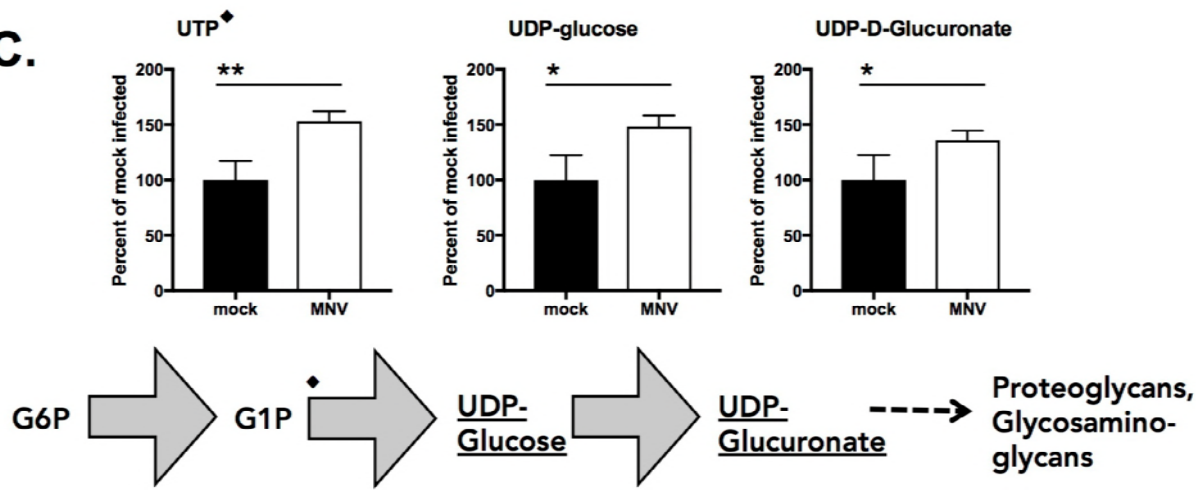


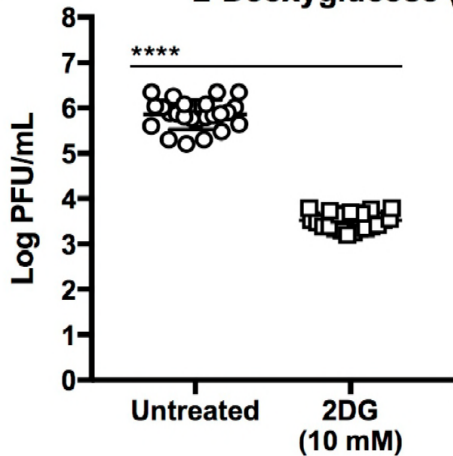
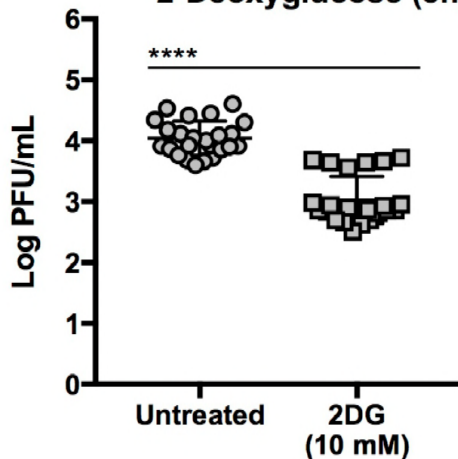
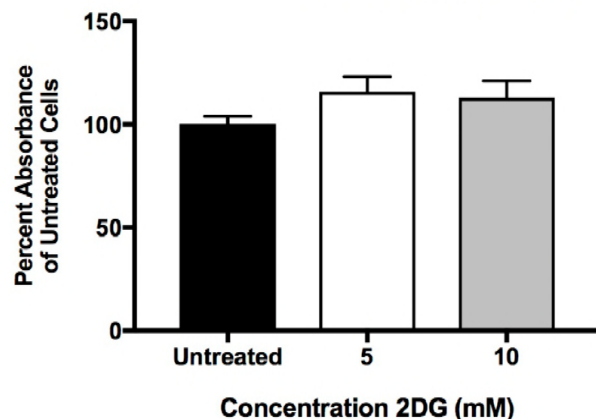
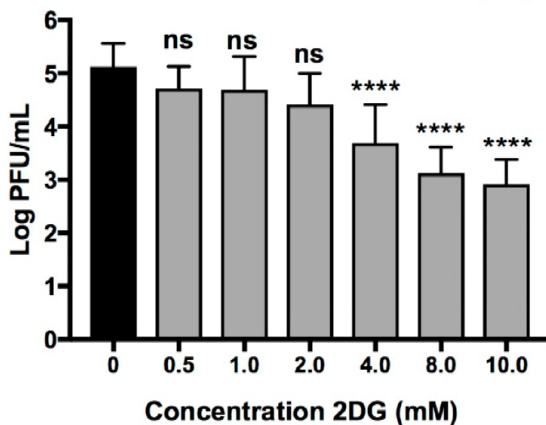
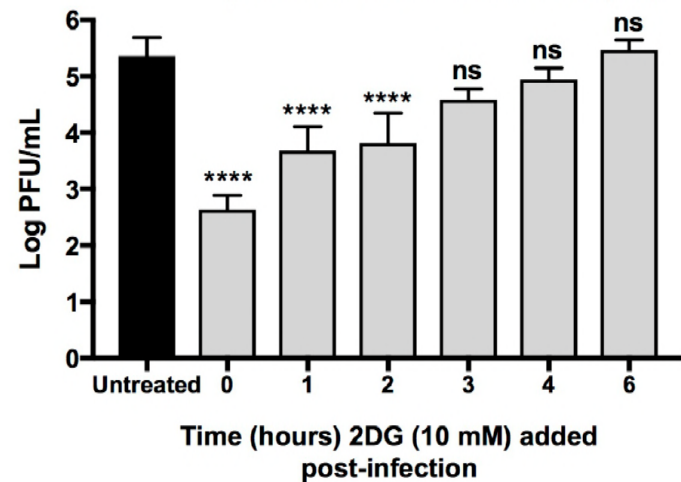
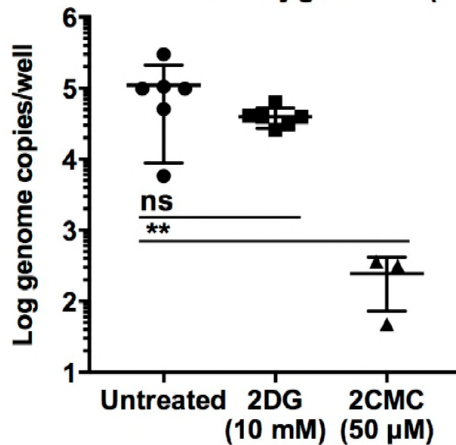
- 714 72. Wieman HL, Wofford JA, Rathmell JC. 2007. Cytokine stimulation promotes glucose  
715 uptake via phosphatidylinositol-3 kinase/Akt regulation of Glut1 activity and trafficking.  
716 *Mol Biol Cell* 18:1437-46.
- 717 73. Vergadi E, Ieronymaki E, Lyroni K, Vaporidi K, Tsatsanis C. 2017. Akt Signaling  
718 Pathway in Macrophage Activation and M1/M2 Polarization. *J Immunol* 198:1006-1014.
- 719 74. Robey RB, Hay N. 2009. Is Akt the "Warburg kinase"?-Akt-energy metabolism  
720 interactions and oncogenesis. *Semin Cancer Biol* 19:25-31.
- 721 75. Matta SK, Kumar D. 2015. AKT mediated glycolytic shift regulates autophagy in  
722 classically activated macrophages. *Int J Biochem Cell Biol* 66:121-33.
- 723 76. Hung YP, Teragawa C, Kosaisawe N, Gillies TE, Pargett M, Minguet M, Distor K,  
724 Rocha-Gregg BL, Coloff JL, Keibler MA, Stephanopoulos G, Yellen G, Brugge JS,  
725 Albeck JG. 2017. Akt regulation of glycolysis mediates bioenergetic stability in epithelial  
726 cells. *Elife* 6.
- 727 77. Kim J, Yang G, Kim Y, Kim J, Ha J. 2016. AMPK activators: mechanisms of action and  
728 physiological activities. *Exp Mol Med* 48:e224.
- 729 78. Faubert B, Boily G, Izreig S, Griss T, Samborska B, Dong Z, Dupuy F, Chambers C,  
730 Fuerth BJ, Viollet B, Mamer OA, Avizonis D, DeBerardinis RJ, Siegel PM, Jones RG.  
731 2013. AMPK is a negative regulator of the Warburg effect and suppresses tumor growth  
732 in vivo. *Cell Metab* 17:113-24.
- 733 79. Dandapani M, Hardie DG. 2013. AMPK: opposing the metabolic changes in both tumour  
734 cells and inflammatory cells? *Biochem Soc Trans* 41:687-93.
- 735 80. Hardie DG. 2008. AMPK: a key regulator of energy balance in the single cell and the  
736 whole organism. *Int J Obes (Lond)* 32 Suppl 4:S7-12.
- 737 81. Winder WW, Holmes BF, Rubink DS, Jensen EB, Chen M, Holloszy JO. 2000.  
738 Activation of AMP-activated protein kinase increases mitochondrial enzymes in skeletal  
739 muscle. *J Appl Physiol* (1985) 88:2219-26.
- 740 82. Merrill GF, Kurth EJ, Hardie DG, Winder WW. 1997. AICA riboside increases AMP-  
741 activated protein kinase, fatty acid oxidation, and glucose uptake in rat muscle. *Am J*  
742 *Physiol* 273:E1107-12.
- 743 83. Gowans GJ, Hardie DG. 2014. AMPK: a cellular energy sensor primarily regulated by  
744 AMP. *Biochem Soc Trans* 42:71-5.
- 745 84. Roberts DJ, Tan-Sah VP, Smith JM, Miyamoto S. 2013. Akt phosphorylates HK-II at  
746 Thr-473 and increases mitochondrial HK-II association to protect cardiomyocytes. *J Biol*  
747 *Chem* 288:23798-806.
- 748 85. Dunn EF, Connor JH. 2012. HijAkt: The PI3K/Akt pathway in virus replication and  
749 pathogenesis. *Prog Mol Biol Transl Sci* 106:223-50.
- 750 86. Lateef Z, Gimenez G, Baker ES, Ward VK. 2017. Transcriptomic analysis of human  
751 norovirus NS1-2 protein highlights a multifunctional role in murine monocytes. *BMC*  
752 *Genomics* 18:39.
- 753 87. Sen S, Kaminiski R, Deshmane S, Langford D, Khalili K, Amini S, Datta PK. 2015. Role  
754 of hexokinase-1 in the survival of HIV-1-infected macrophages. *Cell Cycle* 14:980-9.
- 755 88. Martinez FO, Gordon S. 2014. The M1 and M2 paradigm of macrophage activation: time  
756 for reassessment. *F1000Prime Rep* 6:13.
- 757 89. Van den Bossche J, O'Neill LA, Menon D. 2017. Macrophage Immunometabolism:  
758 Where Are We (Going)? *Trends Immunol* 38:395-406.

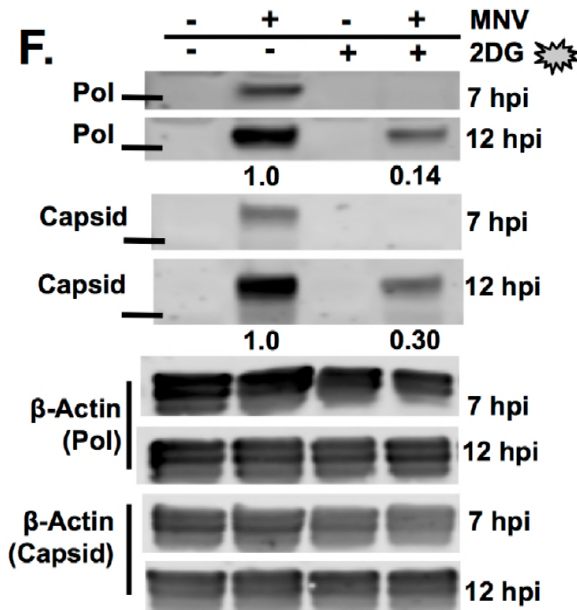
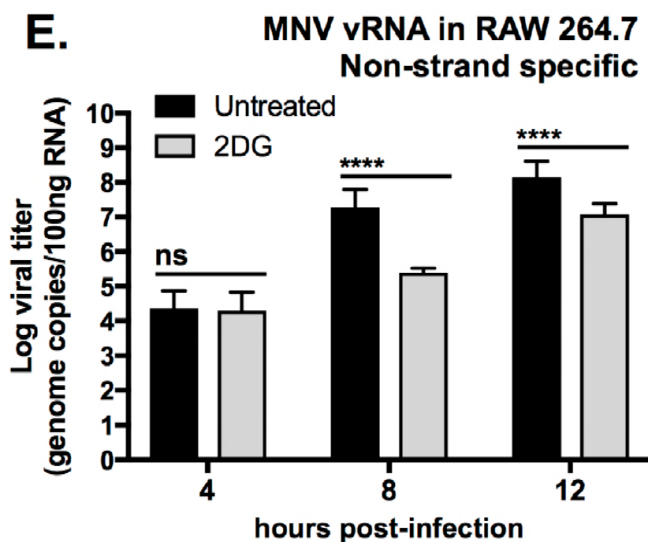
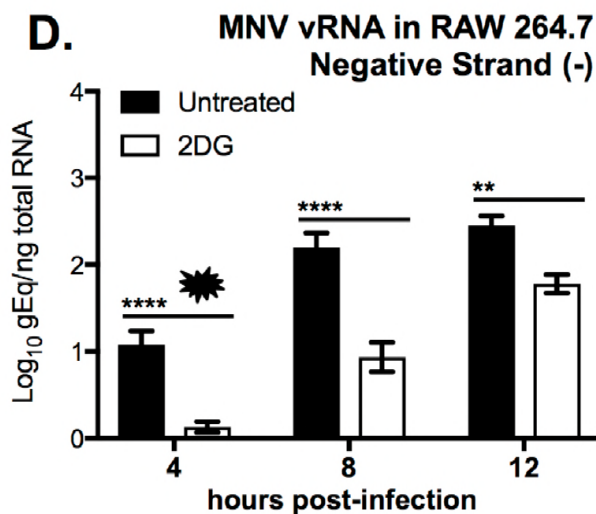
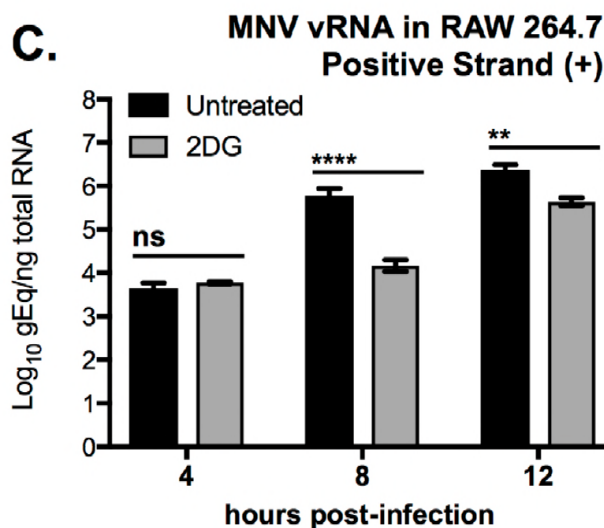
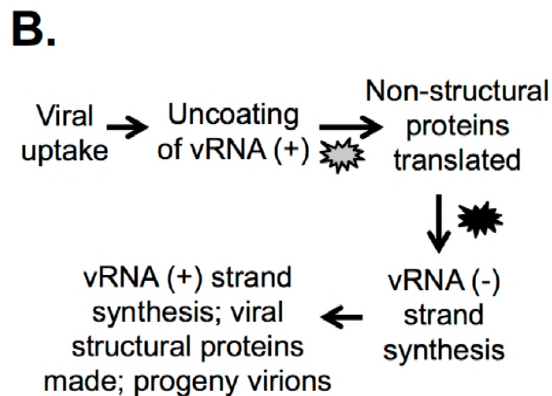
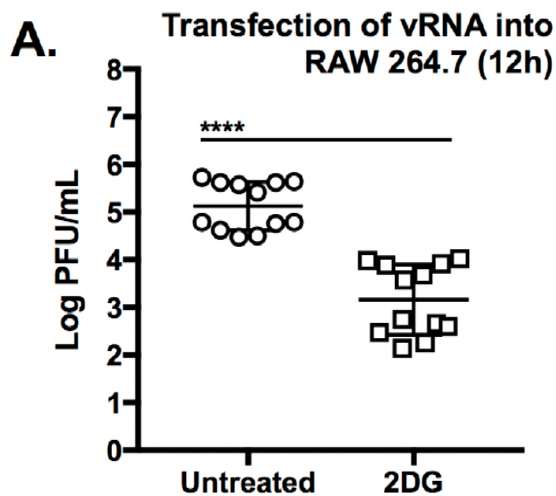
- 759 90. Grau KR, Roth AN, Zhu S, Hernandez A, Colliou N, DiVita BB, Philip DT, Riffe C,  
760 Giasson B, Wallet SM, Mohamadzadeh M, Karst SM. 2017. The major targets of acute  
761 norovirus infection are immune cells in the gut-associated lymphoid tissue. *Nat Microbiol*  
762 2:1586-1591.
- 763 91. Wang Q, Liang B, Shirwany NA, Zou MH. 2011. 2-Deoxy-D-glucose treatment of  
764 endothelial cells induces autophagy by reactive oxygen species-mediated activation of the  
765 AMP-activated protein kinase. *PLoS One* 6:e17234.
- 766 92. Wang A, Huen SC, Luan HH, Yu S, Zhang C, Gallezot JD, Booth CJ, Medzhitov R.  
767 2016. Opposing Effects of Fasting Metabolism on Tissue Tolerance in Bacterial and  
768 Viral Inflammation. *Cell* 166:1512-1525 e12.
- 769 93. Wang Y, Li JR, Sun MX, Ni B, Huan C, Huang L, Li C, Fan HJ, Ren XF, Mao X. 2014.  
770 Triggering unfolded protein response by 2-Deoxy-D-glucose inhibits porcine epidemic  
771 diarrhea virus propagation. *Antiviral Res* 106:33-41.
- 772 94. Ettayebi K, Crawford SE, Murakami K, Broughman JR, Karandikar U, Tenge VR, Neill  
773 FH, Blutt SE, Zeng XL, Qu L, Kou B, Opekun AR, Burrin D, Graham DY, Ramani S,  
774 Atmar RL, Estes MK. 2016. Replication of human noroviruses in stem cell-derived  
775 human enteroids. *Science* 353:1387-1393.
- 776 95. Bartnicki E, Cunha JB, Kolawole AO, Wobus CE. 2017. Recent advances in  
777 understanding noroviruses. *F1000Res* 6:79.
- 778 96. Gonzalez-Hernandez MB, Bragazzi Cunha J, Wobus CE. 2012. Plaque assay for murine  
779 norovirus. *J Vis Exp* doi:10.3791/4297:e4297.
- 780 97. Perry JW, Ahmed M, Chang KO, Donato NJ, Showalter HD, Wobus CE. 2012. Antiviral  
781 activity of a small molecule deubiquitinase inhibitor occurs via induction of the unfolded  
782 protein response. *PLoS Pathog* 8:e1002783.
- 783

**A.**

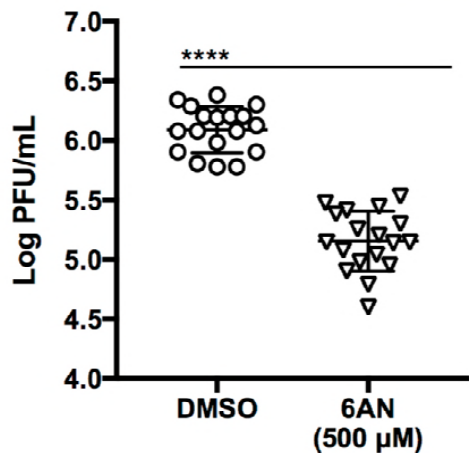


**B.****C.**

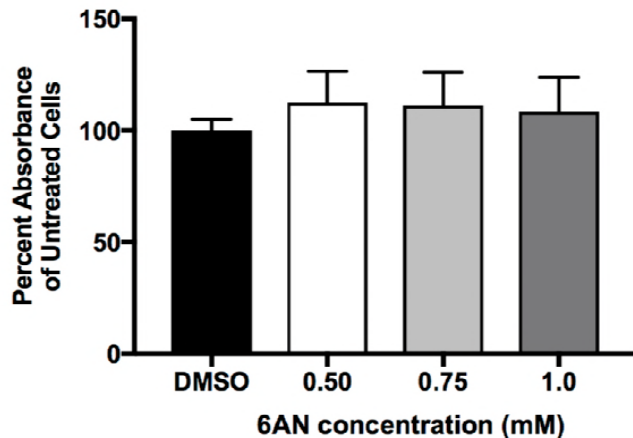
**A.** MNV in RAW 264.7  
2-Deoxyglucose (8h)**B.** MNV in BMDM  
2-Deoxyglucose (8h)**C.** RAW 264.7 Cell Viability  
2-Deoxyglucose (8h)**D.** MNV in RAW 264.7 w/2DG  
variable concentrations (8h)**E.** MNV in RAW 264.7 w/2DG  
post-infection treatment (8h)**F.** Human astrovirus in Caco-2  
2-Deoxyglucose (24h)



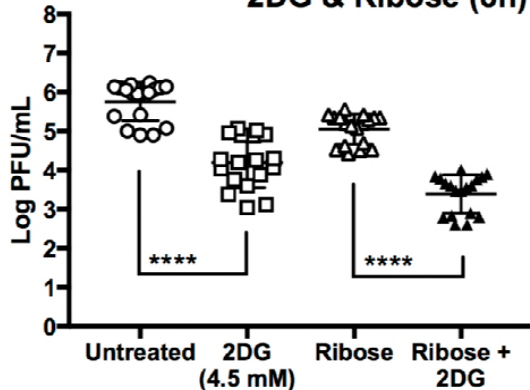
**A.** MNV in RAW 264.7  
6-Aminonicotinamide (8h)



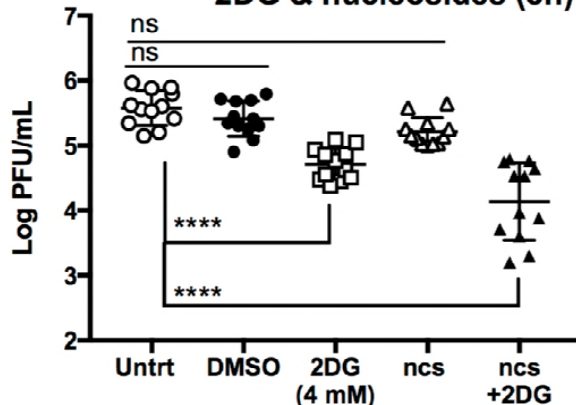
**B.** RAW 264.7 Cell Viability  
6-Aminonicotinamide (8h)



**C.** MNV in RAW 264.7  
2DG & Ribose (8h)



**D.** MNV in RAW 264.7  
2DG & nucleosides (8h)



**MNV in BMDM (8h)  
2-Deoxyglucose (2DG) (10 mM)**

